Refined Analytical Approximations to Limit Cycles for Non-Linear Multi-Degree-of-Freedom Systems

A. P. Lewis

School of Engineering and Technology, University of Hertfordshire, Hatfield, Hertfordshire AL10 9AB, United Kingdom. E-mail: a.lewis@herts.ac.uk

ABSTRACT

This paper presents analytical higher order approximations to limit cycles of an autonomous multi-degree-of-freedom system based on an integro-differential equation method for obtaining periodic solutions to nonlinear differential equations. The stability of the limit cycles obtained was then investigated using a method for carrying out Floquet analysis based on developments to extensions of the method for solving Hill's Determinant arising in analysing the Mathieu equation, which have previously been reported in the literature. The results of the Floquet analysis, together with the limit cycle predictions, have then been used to provide some estimates of points on the boundary of the domain of attraction of stable equilibrium points arising from a sub-critical Hopf bifurcation. This was achieved by producing a local approximation to the stable manifold of the unstable limit cycle that occurs.

The integro-differential equation to be solved for the limit cycles involves no approximations. These only arise through the iterative approach adopted for its solution in which the first approximation is that which would be obtained from the harmonic balance method using only fundamental frequency terms. The higher order approximations are shown to give significantly improved predictions for the limit cycles for the cases considered. The Floquet analysis based approach to predicting the boundary of domains of attraction met with some success for conditions just following a sub-critical Hopf bifurcation.

Although this study has focussed on cubic non-linearities, the method presented here could equally be used to refine limit cycle predictions for other non-linearity types.

KEYWORDS: Limit cycle oscillations; Floquet Analysis; Stability Domains

This research did not receive any specific grant from funding agencies in the public, commercial, or not-for-profit sectors.

1. Introduction

Methods for the analysis of non-linear autonomous systems of ordinary differential equations have been the subject of considerable investigation over many years, from both a purely theoretical viewpoint but also in the context of practical applications. Non-linear ordinary differential equations may, of course, be solved numerically in the time domain. However, a drawback with this is that though it can yield a complete picture of system behaviour for a given set of initial conditions, it can be inefficient in providing an overall picture of system characteristics. Besides this, for non-linear autonomous systems that arise in practical applications, it is generally necessary to solve them for a wide range of system parameters. Analysis based on averaging or other methods of asymptotic analysis has the advantage of being able to yield both qualitative, and in many cases the most important quantitative, information about the system response relatively rapidly, thus enabling an understanding of the system's behaviour to be obtained more quickly. Of particular interest is the determination of limit cycles and their stability for autonomous systems. The literature on analytical methods for solving nonlinear systems is extensive and includes classical perturbation methods such as the Krylov-Bogoliubov, Krylov-Bogoliubov-Mitropolsky methods and generalised averaging [1, 2]. Other approaches which combine analytical and numerical techniques include perturbation-

incremental and perturbation-iterative methods [3 - 6]. There is a very large body of literature on wholly numerically-based approaches based on the harmonic balance method, very many concerned with development of algorithms, for example [7 – 15] while many are also concerned with applications, in particular in the field of non-linear aeroelasticity [16 – 26]. Other methods that have been developed are the differential transform method [27], the application of Floquet analysis as a computational tool for determining periodic solutions [28], and He's homotopy method [29].

In this paper, an analytical approach is taken, the basis of which is the method of Schmidt and Schulz [30] which is then extensively applied in the text by Schmidt and Tondl [31]. The idea of this method is to turn the problem of finding periodic solutions of a non-linear system, including limit cycles, into an integro-differential equation which can then be solved by a Picard iteration approach starting with an approximate initial trial solution. In [31], weak non-linearities tend to be assumed in obtaining higher approximations. In this paper, this same iterative approach is applied, but no smallness assumptions are made. Having obtained approximations to the limit cycles of the non-linear system, Floquet analysis is applied to investigate their stability. The approach taken is to extend to a two degree-of-freedom second order, or equivalently, a four degree-of-freedom first order system, a method applied by Bonani [32] to Chua's circuit, which is a three degree-of-freedom system. This in turn is based on the method for solving Hill's Determinant arising in analysing the Mathieu equation [33]. Limit cycles appear as a consequence of a Hopf bifurcation. In particular, for a sub-critical Hopf bifurcation, an unstable equilibrium point becomes stable and is accompanied by an unstable limit cycle. For such unstable limit cycles, the results of the Floquet analysis then enable a local approximation to the stable manifold of the limit cycle to be found, from which information about the domain of attraction of the stable equilibrium point can be obtained, which may then be compared with time domain predictions. The particular case studied here is a two degree-of-freedom second order system with a cubic non-linearity based on an aeroelastic analysis of an all-moving control surface in supersonic flow where piston theory aerodynamics [34] may be applied. The layout of the paper is as follows: Section 2 outlines the general approach adopted for obtaining periodic solutions, including limit cycles, to a non-linear system. Section 3 derives higher order approximations to the limit cycles of the second order two-degree-of-freedom system with a cubic non-linearity. Section 4 presents the approach taken to stability analysis of the limit cycles via Floquet theory. Section 5 describes how to obtain a local approximation to the stable manifold of an unstable limit cycle and hence information on the domain of stability of a stable equilibrium point of the system following a sub-critical Hopf bifurcation. Sections 6 and 7 present results and Section 8 Concluding Remarks.

2. Integro-Differential Equation Method

The fundamental approach adopted here to determining approximations to limit cycles is based on the result in [30], [31] which may be expressed for a single degree of freedom system of the form:

$$y'' + \lambda y = \Phi(y, y', \tau) \tag{1}$$

as follows. Every periodic solution of (1) is a solution of the integro-differential equation:

$$y(\tau) = \int_0^{2\pi} G(\tau, \sigma)\, \Phi(\sigma) d\sigma + \delta_\lambda^{n^2}(r\cos n\tau + s\sin n\tau) \tag{2}$$

where:

$$G(\tau, \sigma) = \frac{1}{\pi}\left[\frac{1}{2\lambda} + \sum_{\nu=1}^{\infty} \frac{\cos\nu(\tau - \sigma)}{(1 - \delta_\lambda^{n^2})\lambda - \nu^2}\right] \tag{3}$$

and $\delta_\lambda^{n^2}$ is the Kroneker Delta.

The values of *r* and *s*, which arise in the resonance case $\lambda = n^2$ may be obtained from the conditions:

$$\int_0^{2\pi} \Phi(\tau)\cos n\tau \, d\tau = \int_0^{2\pi} \Phi(\tau)\sin n\tau \, d\tau = 0 \tag{4}$$

This result is derived in [31] and embraces both resonance and non-resonance cases. Equations (4) are the conditions for removing the secular terms which arise in the resonance case and effectively lead to the removal of the terms for $\nu = n$ in the summation in Equation (3). [30] and [31] also give equivalent statements to Equations (2), (3) and (4) for the multi-degree-of-freedom case.

Equation (2) may now be solved by an iterative method whereby an appropriate initial form for *y* is assumed in the righthand side of (2) resulting in a refined *y*. The question of the conditions under which convergence to the solution of (2) occurs is considered in [31]. However, it will become apparent when the method is applied whether convergence is occurring.

It might be noted that Hu and Tang [35] also developed a convolution integral method for conservative second order single degree-of-freedom systems with strong nonlinearities where solutions are obtained by an iterative method.

3. Application

The integro-differential equation method of [30], [31] outlined in Section 2 is now applied to the following autonomous nonlinear system:

$$\ddot{\mathbf{X}} + \mathbf{G}\dot{\mathbf{X}} + \mathbf{H}\mathbf{X} + \varepsilon \mathbf{s} f(\mathbf{r}^T\mathbf{X}) = \mathbf{0} \tag{5}$$

where **X** is an *n*-dimensional column vector of dependent variables, **G** and **H** are *n* by *n* damping and stiffness matrices which are not necessarily symmetric, as might be the case in aeroelastic applications, for example. ε governs the strength of the nonlinearity which is characterised by the function *f*. **r**, **s** are *n*-dimensional constant vectors. Derivatives are with respect to time *t*. A non-dimensional time τ is now introduced where $\tau = \omega t$, ω being the frequency of the periodic solution of (5) being sought. Equation (5) is now rewritten:

$$\mathbf{X}'' + \mathbf{X} = \mathbf{\Phi}(\mathbf{X}, \mathbf{X}') \tag{6}$$

where $'$ denotes differentiation with respect to τ, and:

$$\mathbf{\Phi}(\mathbf{X}, \mathbf{X}') = -\frac{1}{\omega}\mathbf{G}\mathbf{X}' - \left(\frac{1}{\omega^2}\mathbf{H} - \mathbf{I}\right)\mathbf{X} - \frac{\varepsilon \mathbf{s}}{\omega^2} f(\mathbf{r}^T\mathbf{X}) \tag{7}$$

As a starting point, a first approximation for **X** is taken as:

$$\mathbf{X}_1 = \boldsymbol{\xi} sin\tau + \boldsymbol{\eta} cos\tau \tag{8}$$

where, given that the system (5) is autonomous, $\boldsymbol{\xi}$ and $\boldsymbol{\eta}$ may, without loss of generality be written as:

$$\mathbf{r}^T\boldsymbol{\xi} = \mathbf{r}^T\boldsymbol{\eta} = \frac{A}{\sqrt{2}} \tag{9}$$

so that A denotes the amplitude of the motion defined by Equation (8). In the remaining part of this Section, periodic solutions of (5) are obtained for the cubic nonlinearity.

For a cubic nonlinearity the function f in equation (5) is defined by:

$$f(\mathbf{r}^T\mathbf{X}) = K(\mathbf{r}^T\mathbf{X})^3 \tag{10}$$

The reason for introducing a perhaps seemingly unnecessary parameter K will become apparent when results are presented in Section 6.

Substituting (8) and (10) into (7) and making use of (9) results in:

$$\begin{aligned}\boldsymbol{\Phi} = -\sin\tau\left\{\left(\frac{1}{\omega^2}\mathbf{H} - \mathbf{I}\right)\boldsymbol{\xi} - \frac{1}{\omega}\mathbf{G}\boldsymbol{\eta}\right\} - \cos\tau\left\{\left(\frac{1}{\omega^2}\mathbf{H} - \mathbf{I}\right)\boldsymbol{\eta} + \frac{1}{\omega}\mathbf{G}\boldsymbol{\xi}\right\} \\ -\frac{K\varepsilon\mathbf{s}}{\omega^2}\frac{A^3}{4\sqrt{2}}\{3(\sin\tau + \cos\tau) + \sin 3\tau - \cos 3\tau\}\end{aligned} \tag{11}$$

Applying the condition to eliminate secular terms (4) gives:

$$\begin{aligned}\left(\frac{1}{\omega^2}\mathbf{H} - \mathbf{I}\right)\boldsymbol{\xi} - \frac{1}{\omega}\mathbf{G}\boldsymbol{\eta} + \frac{\varepsilon K\mathbf{s}}{\omega^2}\frac{3A^3}{4\sqrt{2}} = \mathbf{0} \\ \left(\frac{1}{\omega^2}\mathbf{H} - \mathbf{I}\right)\boldsymbol{\eta} + \frac{1}{\omega}\mathbf{G}\boldsymbol{\xi} + \frac{\varepsilon K\mathbf{s}}{\omega^2}\frac{3A^3}{4\sqrt{2}} = \mathbf{0}\end{aligned} \tag{12}$$

Equations (12) may then be combined to give:

$$\left(\frac{1}{\omega^2}\mathbf{H} - \mathbf{I}\right)(\boldsymbol{\xi} + i\boldsymbol{\eta}) + \frac{i}{\omega}\mathbf{G}(\boldsymbol{\xi} + i\boldsymbol{\eta}) + \frac{\varepsilon K\mathbf{s}}{\omega^2}\frac{3A^3}{4\sqrt{2}}(1 + i) = 0 \tag{13}$$

Making use of Equations (9), Equations (13) may then be written as:

$$\left[\left(\frac{1}{\omega^2}\mathbf{H} - \mathbf{I}\right) + \frac{i}{\omega}\mathbf{G} + \frac{3\varepsilon KA^2}{4\omega^2}\mathbf{s}\mathbf{r}^T\right](\boldsymbol{\xi} + i\boldsymbol{\eta}) = 0 \tag{14}$$

The following determinantal equation is then solved for A and ω:

$$\left|\left(\frac{1}{\omega^2}\mathbf{H} - \mathbf{I}\right) + \frac{i}{\omega}\mathbf{G} + \frac{3\varepsilon KA^2}{4\omega^2}\mathbf{s}\mathbf{r}^T\right| = 0 \tag{15}$$

For the particular case when $n = 2$, the following two equations for A and ω then result:

$$\omega^2(G_{11}+G_{22})-G_{11}H_{22}-G_{22}H_{11}+G_{21}H_{12}+G_{12}H_{21}$$
$$-\frac{3}{4}A^2\varepsilon K(G_{11}s_2r_2+G_{22}s_1r_1-G_{21}s_1r_2-G_{12}s_2r_1)=0 \tag{16}$$

$$\omega^4-\omega^2\left[H_{11}+H_{22}+\frac{3}{4}\varepsilon KA^2(s_1r_1+s_2r_2)+G_{11}G_{22}-G_{12}G_{21}\right]$$
$$+H_{11}H_{22}-H_{21}H_{12}+\frac{3}{4}\varepsilon KA^2(H_{22}s_1r_1+H_{11}s_2r_2-H_{12}s_2r_1-H_{21}s_1r_2)=0 \tag{17}$$

Equations (16) and (17) may then be solved for A and ω. Several points should be noted: (i) these equations are the same as would result from applying harmonic balance, (ii) ω^2 and εA^2 are functions of **G**, **H**, **r** and **s** only, (iii) ω^2 is found from a quadratic equation, implying that up to two limit cycle oscillations are possible; (iv) the conditions that $\omega^2>0$ and $A^2>0$ will determine the number of limit cycle oscillations, (v) for given A and ω, Equation (13) may be used in conjunction with Equations (9) to determine $\boldsymbol{\xi}$ and $\boldsymbol{\eta}$. The first approximation to any limit cycles is then fully determined.

To obtain a refinement to the first approximation, the solution (8) is substituted into (2), noting that the function $G(\tau,\sigma)$ may be rewritten as:

$$G(\tau,\sigma)=\frac{1}{\pi}\sum_{\nu=1}^{\infty}\frac{\cos(2\nu+1)(\tau-\sigma)}{1-(2\nu+1)^2} \tag{18}$$

since in this case, $\lambda = 1$, and as the nonlinearity is an odd function, only odd trigonometric terms are retained and the terms in $\cos\tau$ and $\sin\tau$ are zero due to Equation (4) being satisfied. Furthermore, only the terms for $\nu = 1$ in Equation (18) and those for $\cos3\tau$ and $\sin3\tau$ in Equation (11) will contribute to the refined approximation for $\mathbf{X}_{1r}$, which may then be determined from:

$$\mathbf{X}_{1r}=\boldsymbol{\xi}sin\tau+\boldsymbol{\eta}cos\tau+\frac{1}{\pi}\frac{\varepsilon K\mathbf{s}}{\omega^2}\frac{A^3}{4\sqrt{2}}\int_0^{2\pi}\frac{\cos3\sigma\cos3\tau+\sin3\sigma\sin3\tau}{8}\{sin3\sigma-cos3\sigma\}d\sigma \tag{19}$$

Hence $\mathbf{X}_{1r}$, the refined first approximation is:

$$\mathbf{X}_{1r}=\boldsymbol{\xi}sin\tau+\boldsymbol{\eta}cos\tau-\frac{\varepsilon K\mathbf{s}}{\omega^2}\frac{A^3}{32\sqrt{2}}\{cos3\tau-sin3\tau\} \tag{20}$$

To obtain the next solution estimate, $\mathbf{X}_{1r}$ from equation (20) is substituted into (7) to give:

$$\boldsymbol{\Phi}=-\sin\tau\left\{\left(\frac{1}{\omega^2}\mathbf{H}-\mathbf{I}\right)\boldsymbol{\xi}-\frac{1}{\omega}\mathbf{G}\boldsymbol{\eta}\right\}-\cos\tau\left\{\left(\frac{1}{\omega^2}\mathbf{H}-\mathbf{I}\right)\boldsymbol{\eta}+\frac{1}{\omega}\mathbf{G}\boldsymbol{\xi}\right\}$$
$$-\frac{\varepsilon K\mathbf{s}}{\omega^2}\frac{3A^3}{4\sqrt{2}}(1+\beta A^2+2\beta^2A^4)(\sin\tau+\cos\tau)+\cdots.. \tag{21}$$

where only the terms in cosτ and sinτ are given. β is given by:

$$\beta = \frac{\varepsilon K \mathbf{r}^T \mathbf{s}}{32\omega^2} \tag{22}$$

Applying the condition (4) to eliminate secular terms then gives:

$$\left[\left(\frac{1}{\omega^2}\mathbf{H} - \mathbf{I}\right) + \frac{i}{\omega}\mathbf{G} + \frac{3\varepsilon K A^2}{4\omega^2}(1 + \beta A^2 + 2\beta^2 A^4)\mathbf{s}\mathbf{r}^T\right](\boldsymbol{\xi} + i\boldsymbol{\eta}) = 0 \tag{23}$$

and the following determinantal equation is then solved for A and ω:

$$\left|\left(\frac{1}{\omega^2}\mathbf{H} - \mathbf{I}\right) + \frac{i}{\omega}\mathbf{G} + \frac{3\varepsilon K A^2}{4\omega^2}(1 + \beta A^2 + 2\beta^2 A^4)\mathbf{s}\mathbf{r}^T\right| = 0 \tag{24}$$

The following two equations for A and ω then result:

$$\begin{aligned}&\omega^2(G_{11} + G_{22}) - G_{11}H_{22} - G_{22}H_{11} + G_{21}H_{12} + G_{12}H_{21} \\ &\quad -\frac{3}{4}K\varepsilon A^2(1 + \beta A^2 + 2\beta^2 A^4)(G_{11}s_2r_2 + G_{22}s_1r_1 - G_{21}s_1r_2 - G_{12}s_2r_1) = 0\end{aligned} \tag{25}$$

$$\begin{aligned}&\omega^4 - \omega^2\left[H_{11} + H_{22} + \frac{3}{4}K\varepsilon A^2(1 + \beta A^2 + 2\beta^2 A^4)(s_1r_1 + s_2r_2)\right] \\ &\quad +G_{11}G_{22} - G_{12}G_{21} + H_{11}H_{22} - H_{21}H_{12} \\ &\quad +\frac{3}{4}K\varepsilon A^2(1 + \beta A^2 + 2\beta^2 A^4)(H_{22}s_1r_1 + H_{11}s_2r_2 - H_{12}s_2r_1 - H_{21}s_1r_2) = 0\end{aligned} \tag{26}$$

These equations may be solved for ω by eliminating the function of A, $\varepsilon K A^2(1 + \beta A^2 + 2\beta^2 A^2)$, which will result in the same equation for ω as for the first approximation.

Thus the Equation for A will be a cubic in A^2 of the form:

$$p(A^2) = A^6 + \frac{1}{2\beta}A^4 + \frac{1}{2\beta^2}A^2 + B(\omega) = 0 \tag{27}$$

It may be readily shown that (27) only has one real root, as the function $p(A^2)$, regarded as a cubic in A^2, has no turning points, and hence will yield at most one value of A for a given ω. The resulting

value of A may be used in Equation (20) to give a second approximation and $\boldsymbol{\xi}$ and $\boldsymbol{\eta}$ may in turn be updated.

Substituting Equation (20) into (7) and noting that Equations (4) need to be satisfied gives:

$$\begin{aligned}\boldsymbol{\Phi} = \cos 3\tau &\left\{-\frac{3K\epsilon}{\omega^3}\frac{A^3}{32\sqrt{2}}\mathbf{Gs} + \frac{3K\epsilon}{\omega^2}\frac{A^3}{32\sqrt{2}}\left(\frac{1}{\omega^2}\mathbf{H} - \mathbf{I}\right)\mathbf{s} - \frac{K\epsilon}{\omega^2}\frac{A^3}{\sqrt{2}}S_3\mathbf{s}\right\} \\ &+ \sin 3\tau\left\{-\frac{3K\epsilon}{\omega^3}\frac{A^3}{32\sqrt{2}}\mathbf{Gs} - \frac{3K\epsilon}{\omega^2}\frac{A^3}{32\sqrt{2}}\left(\frac{1}{\omega^2}\mathbf{H} - \mathbf{I}\right)\mathbf{s} - \frac{K\epsilon}{\omega^2}\frac{A^3}{\sqrt{2}}S_3\mathbf{s}\right\} \\ &+ \frac{K\epsilon}{\omega^2}\frac{A^3}{\sqrt{2}}S_5(cos5\tau + sin5\tau)\mathbf{s} + \frac{K\epsilon}{\omega^2}\frac{A^3}{\sqrt{2}}S_7(cos7\tau - sin7\tau)\mathbf{s} \\ &- \frac{K\epsilon}{\omega^2}\frac{A^3}{\sqrt{2}}S_9(cos9\tau + sin9\tau)\mathbf{s}\end{aligned} \tag{28}$$

where:

$$\begin{aligned}S_3 = -\left\{\frac{1}{4} + \frac{3}{2}\beta A^2 + \frac{3}{4}\beta^3 A^6\right\};\ \ S_5 = \frac{3}{4}\beta\{A^2 + \beta A^4\} \\ S_7 = -\frac{3}{4}\beta^2 A^4;\quad S_9 = \frac{1}{4}\beta^3 A^6\end{aligned} \tag{29}$$

Hence $\boldsymbol{\Phi}$ can be written in the form:

$$\boldsymbol{\Phi} = \mathbf{U}_3\cos 3\tau + \mathbf{V}_3\sin 3\tau + \mathbf{U}_5\cos 5\tau + \mathbf{V}_5\sin 5\tau + \mathbf{U}_7\cos 7\tau + \mathbf{V}_7\sin 7\tau + \mathbf{U}_9\cos 9\tau + \mathbf{V}_9\sin 9\tau \tag{30}$$

where $\mathbf{U}_3$, $\mathbf{U}_5$, $\mathbf{U}_7$, $\mathbf{U}_9$, $\mathbf{V}_3$, $\mathbf{V}_5$, $\mathbf{V}_7$, $\mathbf{V}_9$ may be readily identified from Equations (28) and (29). The second refined approximation $\mathbf{X}_{2r}$, may be found by substituting (27) into (2) to give:

$$\begin{aligned}\mathbf{X}_{2r} = \boldsymbol{\xi} sin\tau + \boldsymbol{\eta} cos\tau &- \frac{\mathbf{U}_3}{8}cos3\tau - \frac{\mathbf{V}_3}{8}sin3\tau - \frac{\mathbf{U}_5}{24}cos5\tau - \frac{\mathbf{V}_5}{24}sin5\tau - \frac{\mathbf{U}_7}{48}cos7\tau - \frac{\mathbf{V}_7}{48}sin7\tau \\ &- \frac{\mathbf{U}_9}{80}cos9\tau - \frac{\mathbf{V}_9}{80}sin9\tau\end{aligned} \tag{31}$$

Further refinements may be obtained by repeating the process. This will result in polynomial equations for amplitude A of increasingly higher order (which will need to be solved numerically) and additional terms in the series expansions for the limit cycle approximation. However, for the purposes of this study, the approximations obtained here will suffice.

4. Stability Analysis

The stability of the limit cycles obtained by the method in Section 3 are now determined by extending an approach developed in [32] for the analysis of Chua's circuit, a first order three degree-of-freedom system. It is now assumed that $\mathbf{X}$ represents a limit cycle oscillation of (5) and $\boldsymbol{\Delta}\mathbf{X}$ a small perturbation of the limit cycle. Then to first order, $\boldsymbol{\Delta}\mathbf{X}$, satisfies the equation:

$$\Delta\ddot{\mathbf{X}} + \mathbf{G}\Delta\dot{\mathbf{X}} + \mathbf{H}\Delta\mathbf{X} + \varepsilon\mathbf{s}\mathbf{r}^T f'(\mathbf{r}^T\mathbf{X})\Delta\mathbf{X} = \mathbf{0} \tag{32}$$

Following [32] a solution for $\boldsymbol{\Delta}\mathbf{X}$ is now sought by writing:

$$\Delta\mathbf{X} = \sum_{l=1}^{4} H_l \mathbf{v}_l(t)\, e^{\lambda_l t} \tag{33}$$

where H_l are scalar constants whose values would be dependent on initial conditions, $\boldsymbol{v}_l$ are two-dimensional vector functions of period $2\pi/\omega$ and the λ_l are complex numbers which will determine the stability of the limit cycle.

Denoting by $\mathbf{v}(t)$ any of the functions $\mathbf{v}_l(t)$ for l = 1, 2, 3, 4, $\mathbf{v}$ may be written:

$$\mathbf{v}(\tau) = \sum_{k=-\infty}^{+\infty} \mathbf{V}_k\, e^{i\omega k\tau} \tag{34}$$

and writing:

$$\varepsilon \mathbf{s}\mathbf{r}^T f'(\mathbf{r}^T\mathbf{X}) = \sum_{k=-\infty}^{+\infty} \mathbf{G}_k\, e^{i\omega kt} \tag{35}$$

where ω is the known limit cycle frequency and $f'(\mathbf{r}^T\mathbf{X})$ is periodic in ω. $\mathbf{V}_k$ is a two-dimensional column vector and $\mathbf{G}_k$ is 2 by 2 matrix; both have complex elements.

Substituting (33), (34) and (35) into (32) gives:

$$\sum_{k=-\infty}^{+\infty} \{(i\omega+\lambda)^2\mathbf{I} + (i\omega+\lambda)\mathbf{G} + \mathbf{H}\}\mathbf{V}_k\, e^{i\omega kt} + \sum_{k=-\infty}^{+\infty}\sum_{k=-\infty}^{+\infty} \mathbf{G}_l\mathbf{V}_k\, e^{i\omega(k+l)t} = 0 \tag{36}$$

Equating coefficients in $e^{i\omega t}$ then leads to an infinite set of linear simultaneous homogeneous equations in $\mathbf{V}_k$. The requirement for a non-trivial solution to these equations results in the following determinantal equation for λ:

$$\mathrm{Det}(\mathbf{M}) = 0 \tag{37}$$

where Equations (36) have been written as:

$$\mathbf{M}\bar{\mathbf{V}} = \begin{bmatrix} \cdots & \cdots & \cdots & \cdots & \cdots & \cdots & \cdots & \cdots & \cdots & \cdots & \cdots \\ \cdots & \mathbf{G}_\mathrm{N} & \cdots & \mathbf{G}_1 & \widetilde{\mathbf{G}}_{-1} & \mathbf{G}_{-1} & \cdots & \mathbf{G}_{-\mathrm{N}} & \cdots & \cdots & \cdots \\ \cdots & \cdots & \mathbf{G}_\mathrm{N} & \cdots & \mathbf{G}_1 & \widetilde{\mathbf{G}}_0 & \mathbf{G}_{-1} & \cdots & \mathbf{G}_{-\mathrm{N}} & \cdots & \cdots \\ \cdots & \cdots & \cdots & \mathbf{G}_\mathrm{N} & \cdots & \mathbf{G}_1 & \widetilde{\mathbf{G}}_1 & \mathbf{G}_{-1} & \cdots & \mathbf{G}_{-\mathrm{N}} & \cdots \\ \cdots & \cdots & \cdots & \cdots & \cdots & \cdots & \cdots & \cdots & \cdots & \cdots & \cdots \end{bmatrix} \begin{bmatrix} \cdots \\ \cdots \\ \mathbf{V}_{-\mathbf{N}} \\ \cdots \\ \mathbf{V}_{-\mathbf{1}} \\ \mathbf{V}_\mathbf{0} \\ \mathbf{V}_\mathbf{1} \\ \cdots \\ \mathbf{V}_\mathbf{N} \\ \cdots \\ \cdots \end{bmatrix} = \mathbf{0} \tag{38}$$

with:

$$\widetilde{\mathbf{G}}_k = (i\omega k+\lambda)^2\mathbf{I} + (i\omega k+\lambda)\mathbf{G} + \mathbf{H} + \boldsymbol{G}_0 \tag{39}$$

The determinantal equation (37) will have infinitely many solutions of the form $\lambda_l \pm i\omega k$. In principle, Equation (37) could be solved approximately by taking a finite number of rows and columns in the determinant. However, a better approach is to proceed as in [32], which in turn builds on the approach of Whittaker and Watson [33] in the analysis of Mathieu's equation, and define a new matrix $\mathbf{M}_1$ by:

$$\mathbf{M}_1 = \mathrm{diag}\{\widetilde{\mathbf{G}}_k^{-1}\}\mathbf{M} \tag{40}$$

The determinantal equation $\mathrm{Det}(\mathbf{M}_1) = 0$ will have the same roots as (34). However, it will also possess infinitely many simple poles located at $\lambda = \lambda_{s1} \pm i\omega k; \lambda_{s2} \pm i\omega k; \lambda_{s3} \pm i\omega k; \lambda_{s4} \pm i\omega k$, where $\lambda_{s1}, \lambda_{s2}, \lambda_{s3}, \lambda_{s4}$ are solutions of the equation $\mathrm{Det}(\widetilde{\mathbf{G}}_0) = 0$. Furthermore, all poles located at $\lambda_{sl} \pm i\omega k$ for a given l will have the same residue for all k. $\lambda_{s1}, \lambda_{s2}, \lambda_{s3}, \lambda_{s4}$ will be complex conjugate pairs, and so it is then possible to write $\lambda_{s3} = \lambda_{s1}^*, \lambda_{s4} = \lambda_{s2}^*$. One of the solutions of (37) will be $\lambda = 0$, corresponding to the limit cycle, and hence the determinantal equation $\mathrm{Det}(\mathbf{M}_1) = 0$ may be written in terms of a Mittag-Leffler expansion as follows:

$$\mathrm{Det}(\mathbf{M}_1) = \sum_{l=1}^{4} c_l \sum_{k=-\infty}^{+\infty} \left[\frac{1}{\lambda - (\lambda_{sl} + ik\omega)} + \frac{1}{(\lambda_{sl} + ik\omega)}\right] \tag{41}$$

where c_l is the residue of the pole λ_{sl}. (41) may then be written:

$$\mathrm{Det}(\mathbf{M}_1) = \frac{i\omega}{\pi} \sum_{l=1}^{4} c_l \left[\cot\left(\frac{i(\lambda - \lambda_{sl})\pi}{\omega}\right) + \cot\left(\frac{i\lambda_{sl}\pi}{\omega}\right)\right] = 0 \tag{42}$$

In order to determine the residues of $\mathrm{Det}(\mathbf{M}_1)$, first note that this may be written as:

$$\mathrm{Det}(\mathbf{M}_1) = \mathrm{Det}(\mathbf{M}) \prod_{k=-\infty}^{+\infty} \mathrm{Det}\{\widetilde{\mathbf{G}}_k^{-1}\} \tag{43}$$

where the residues arise due to the term $\mathrm{Det}\{\widetilde{\mathbf{G}}_0^{-1}\}$. Details of the determination of these residues may be found in Appendix B.

Equation (42) may be solved by writing, as in [32]:

$$\mu = \exp\left(\frac{2\pi\lambda}{\omega}\right);\ \mu_{sk} = \exp\left(-\frac{2\pi\lambda_{sk}}{\omega}\right); \tag{44}$$

This leads to a quartic equation in μ, where one solution will be $\mu = 1$, so that the remaining values of μ may be found from a cubic equation:

$$a\mu^3 + b\mu^2 + c\mu + d = 0 \tag{45}$$

The values of the coefficients a, b, c, d are given in Appendix C.

5. Local Stable Manifold and Stability Domain Estimation

Following a sub-critical Hopf bifurcation, the stability domain of the stable equilibrium point that arises is given by the stable manifold of the unstable limit cycle [36]. From the analysis in Section 4, the solution of Equations (5) in the neighbourhood of the limit cycle may be written as:

$$\widetilde{\mathbf{X}} = \mathbf{X} + \Delta\mathbf{X} = \mathbf{X} + \sum_{l=1}^{4} H_l \mathbf{v}_l(t)\, e^{\lambda_l t} \tag{46}$$

with $\mathbf{X}$ denoting the limit cycle from Equation (31) and three of the λ_l being determined from Equations (44) and (45) with the remaining λ_l, which corresponds to the limit cycle being 0. If the limit cycle is unstable, one of the other λ_l will be positive. Hence the local stable manifold may be determined from:

$$\widetilde{\mathbf{X}} = \mathbf{X} + \Delta\mathbf{X} = \sum_{l=1}^{2} H_l \mathbf{v}_l(t)\, e^{\lambda_l t} \tag{47}$$

where λ_1, λ_2 will possess negative real parts. Substituting from equation (31) then gives:

$$\widetilde{\mathbf{X}} = \mathbf{X} + H_1 \sum_{k=-\infty}^{+\infty} \mathbf{V}_{1k}\, e^{(i\omega k+\lambda_1)t} + H_2 \sum_{k=-\infty}^{+\infty} \mathbf{V}_{2k}\, e^{(i\omega k+\lambda_2)t} \tag{48}$$

The vectors $\mathbf{V}_{1k}$ and $\mathbf{V}_{2k}$ are obtained from the homogenous simultaneous Equations (38) with $\lambda = \lambda_1$ and $\lambda = \lambda_2$ respectively. In doing so, note that the right hand side of equation (38) is real and so a switch is made from working in complex numbers to working in real numbers. Define the matrix $\mathbf{J}$ as follows:

$$\mathbf{J} = \begin{bmatrix} \dots & \dots & \dots & \dots & \dots & \dots & \dots & \dots & \dots & \dots & \dots \\ \dots & \mathbf{0} & \mathbf{0} & \mathbf{I} & \mathbf{0} & \mathbf{0} & \mathbf{0} & -\mathbf{I}i & \mathbf{0} & \mathbf{0} & \dots \\ \dots & \mathbf{0} & \mathbf{0} & \mathbf{0} & \mathbf{I} & \mathbf{0} & -\mathbf{I}i & \mathbf{0} & \mathbf{0} & \mathbf{0} & \dots \\ \dots & \mathbf{0} & \mathbf{0} & \mathbf{0} & \mathbf{0} & \mathbf{I} & \mathbf{0} & \mathbf{0} & \mathbf{0} & \mathbf{0} & \dots \\ \dots & \mathbf{0} & \mathbf{0} & \mathbf{0} & \mathbf{I} & \mathbf{0} & \mathbf{I}i & \mathbf{0} & \mathbf{0} & \mathbf{0} & \dots \\ \dots & \mathbf{0} & \mathbf{0} & \mathbf{I} & \mathbf{0} & \mathbf{0} & \mathbf{0} & \mathbf{I}i & \mathbf{0} & \mathbf{0} & \dots \\ \dots & \dots & \dots & \dots & \dots & \dots & \dots & \dots & \dots & \dots & \dots \end{bmatrix} \tag{49}$$

where in Equation (49), $\mathbf{I}$ denotes a 2 x 2 identity matrix and $\mathbf{0}$ a 2 x 2 zero matrix. It is then possible to rewrite equation (38) as:

$$\mathbf{J^{-1}M\overline{V}} = \mathbf{J^{-1}MJJ^{-1}\overline{V}} = \mathbf{NJ^{-1}\overline{V}} = \mathbf{NW} = \mathbf{0} \tag{50}$$

Where $\mathbf{N} = \mathbf{J^{-1}MJ}$ will now be a real matrix and hence $\mathbf{W} = \mathbf{J^{-1}\overline{V}}$ will be a real solution to Equations (50).

Suppose $k = N$ terms are taken in the series expansion (33). Then the matrices $\mathbf{M}$ and $\mathbf{N}$ will be $4N+2 \times 4N+2$ and $\mathbf{V}$ and $\mathbf{W}$ will be column vectors of dimension $4N + 2$. Now take some element of $\mathbf{W}$ as

1.0, Equations (50) may then be rewritten to obtain the remaining elements of **W.** The resulting vectors are then taken as $\mathbf{V}_{1k}$ and $\mathbf{V}_{2k}$ in equation (45) for $\lambda = \lambda_1$ and $\lambda = \lambda_2$ respectively.

To determine approximations to points on the stable manifold of the unstable limit cycle, and hence to the stability domain, initial conditions in $d\widetilde{\mathbf{X}}/dt$ may be first specified. A particular point on the limit cycle corresponding to time $\tau_0 = \omega t_0$ can be chosen so that at this point, the initial conditions are satisfied. Thus:

$$\left(\frac{d\widetilde{\mathbf{X}}}{dt}\right)_{t=t_0} = \left(\frac{d\mathbf{X}}{dt}\right)_{t=t_0} + H_1 \sum_{k=-\infty}^{+\infty} \mathbf{V}_{1k}(i\omega k + \lambda_1)\, e^{(i\omega k+\lambda_1)t_0} + H_2 \sum_{k=-\infty}^{+\infty} \mathbf{V}_{2k}\,(i\omega k + \lambda_2) e^{(i\omega k+\lambda_2)t_0} \tag{51}$$

Equations (51) may then be solved for H_1 and H_2. $\widetilde{\mathbf{X}}$ at $\tau_0 = \omega t_0$ may then be determined from equation (47). This process may be repeated for $0 \leq \tau_0 \leq 2\pi$.

6. Limit Cycle Analysis

In this section, examples of limit cycle predictions are given and comparisons with time domain results are made. . In the time domain approach, Equations (5) are solved numerically using a variable step Runge-Kutta method. All the examples are based on an aeroelastic analysis of an all-moving control surface with a non-linearity in the torsional degree-of-freedom of the root support. Supersonic airflow was considered and the aerodynamic loadings were modelled using third order piston theory aerodynamics [34]. Because of the simple form of the aerodynamics arising from the use of piston theory, the resulting aeroelastic equations take the form of Equations (5) with the matrices **G** and **H** being asymmetric and combining aerodynamic and structural damping and stiffness terms. Displacements of the control surface are expressed in terms of its modes of vibration in the absence of the non-linearity so that **X** is a vector of generalised displacements.

In this example, **G** and **H** are given by:

$$\mathbf{G} = \begin{bmatrix} 0.018444 & 0.002490 \\ 0.000398 & 0.018122 \end{bmatrix} + C \begin{bmatrix} 1.8949752 & 2.2453181 \\ 0.3591434 & 0.4255418 \end{bmatrix} \tag{52}$$

$$\mathbf{H} = \begin{bmatrix} 0 & 0 \\ 0 & 1.4107697 \end{bmatrix} + K \begin{bmatrix} 0.105276 & 0.1247399 \\ 0.019952 & 0.0236412 \end{bmatrix} + V \begin{bmatrix} 0.02281027 & 0.02293653 \\ -0.0331607 & -0.0351129 \end{bmatrix} \tag{53}$$

r and **s** are given by:

$$\mathbf{r} = \begin{bmatrix} 1 \\ 1.18488 \end{bmatrix} \qquad \mathbf{s} = \begin{bmatrix} 0.1052764 \\ 0.0199525 \end{bmatrix} \tag{54}$$

Where C, K are parameters related to linear torsional damping and stiffness of the lifting surface support and V is a speed parameter. The nonlinearity parameter ε will be taken as positive throughout (signifying a hardening non-linearity) and characterises a deviation from a linear support stiffness K.

The bifurcational behaviour of the system as C, K and V are varied is first considered. The system (5) has an equilibrium point $\mathbf{X} = 0$. Combinations of C, K and V where the stability of the equilibrium point changes indicate where bifurcations occur, and determining whether limit cycles occur for C, K and V in the neighbourhood of the bifurcation is through using the analysis of Section 3. Their stability is determined using the theory of Section 4 and establishes whether a sub-critical or super-critical Hopf bifurcation occurs.

The bifurcational behaviour of the system is indicated in Fig. 1 in terms of K and V for two values of C. Considering the case $C = 0$, the equilibrium point is unstable for combinations of K and V above the curve and to the left of its minimum. For V below this part of the curve, a sub-critical Hopf bifurcation occurs whereby the equilibrium point becomes stable and an unstable limit cycle appears. On the other hand, the equilibrium point is stable for combinations of K and V below the curve and to the right of its minimum. For V above this part of the curve, a super-critical Hopf bifurcation occurs whereby the equilibrium point becomes unstable and a stable limit cycle appears.

The minimum of the curve, where approximately, $K = 8$ and $V = 6$, corresponds to a co-dimension 2 bifurcation where the stable equilibrium point becomes unstable and a stable and unstable limit cycle appear simultaneously.

A similar pattern of behaviour occurs for $C = 0.1$ as can also be seen in Fig. 1.

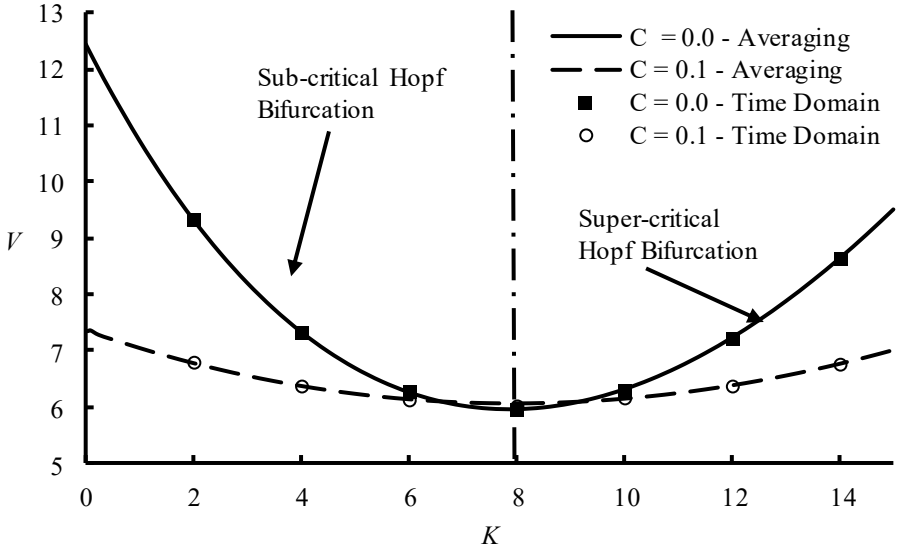

Fig. 1 Bifurcational Behaviour of Nonlinear System

The bifurcational behaviour of the system is also illustrated in Table 1, which summarises limit cycle characteristics for combinations of K and V for $C = 0$ in terms of amplitude of the fundamental frequency component, fundamental frequency and maximum modulus of the Floquet exponent. The behaviour of the system was also confirmed through time domain analysis as indicated in Fig. 1. It will be noted that for $K < 8$ two limit cycles occur (one stable and one unstable) arise.

K	V	A_1	ω_1	max (μ_1)	A_2	ω_2	max (μ_2)
1	10	0.515	0.872	2.536	2.675	1.273	0.954
3	8	0.194	0.935	1.522	1.309	1.219	0.951
5	6	0.474	1.060	1.432	0.617	1.102	0.940
7	6	0.099	1.060	1.069	0.351	1.102	0.940
9	7	-	-	-	0.390	1.180	0.949
11	7	-	-	-	0.171	1.180	0.948
13	8	-	-	-	0.086	1.219	0.947

Table 1. Illustration of Limit Cycle Behaviour Following Hopf Bifurcation

A number of examples of limit cycles determined by the method of Section 3 and time domain analysis are now presented to indicate the effectiveness of the method.

As a first example, limit cycle predictions are shown in Figs. 2 to 5 for the case $K = 0.5$, $V = 6.9$, $C = 0$, $\varepsilon = 2.5$. Fig. 2 compares the time domain prediction and first approximation for the unstable limit cycle, while Figs. 3 to 5 show results for the stable limit cycle using the first approximation, first refined approximation and second refined approximation. For the unstable limit cycle, where the amplitudes of motion are small, the first approximation is very accurate. This is not the case for the stable limit cycle and Fig. 3 shows the influence of higher harmonics on the limit cycle are quite significant. Figs. 4 and 5 show that the first refined approximation gives a significant improvement and the second refined approximation gives still closer agreement with time domain predictions. Figures 6 to 8 show the corresponding results where now $C = 0.1$.

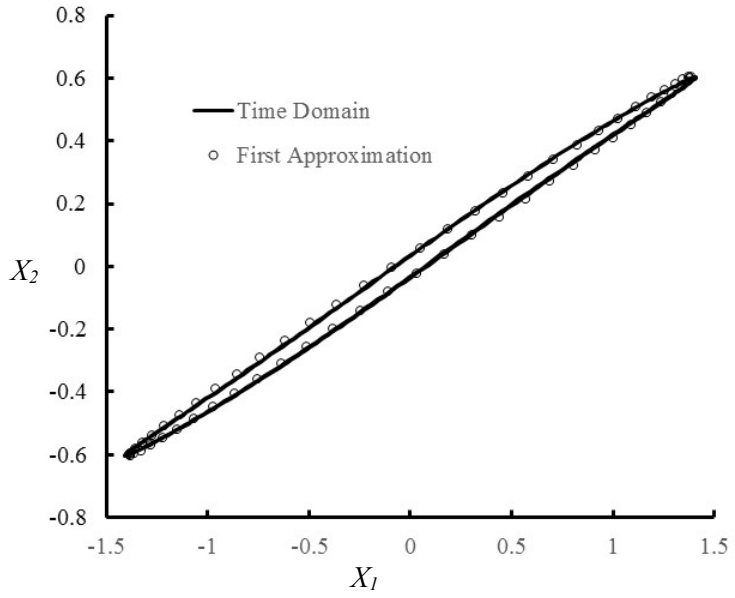

Fig. 2 First Approximation Unstable Limit Cycle Prediction. $K = 0.5$, $V = 6.9$, $C = 0$, $\varepsilon = 2.5$

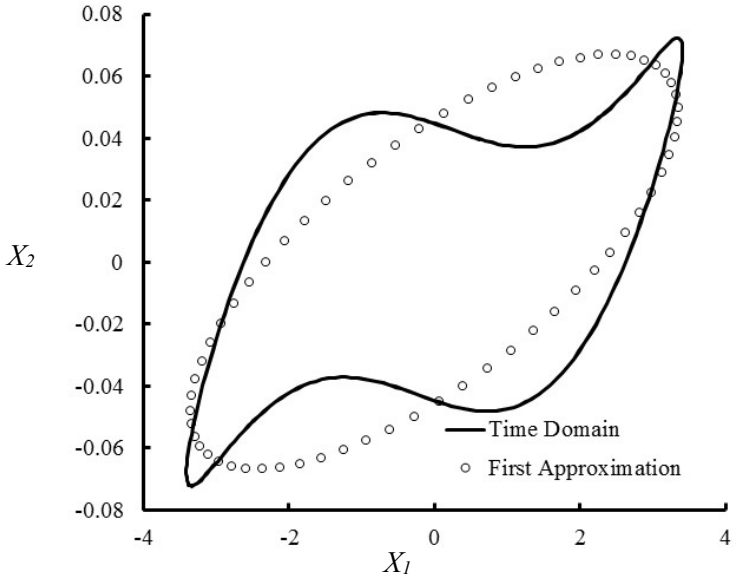

Fig. 3 First Approximation Stable Limit Cycle Prediction. $K = 0.5$, $V = 6.9$, $C = 0$, $\varepsilon = 2.5$

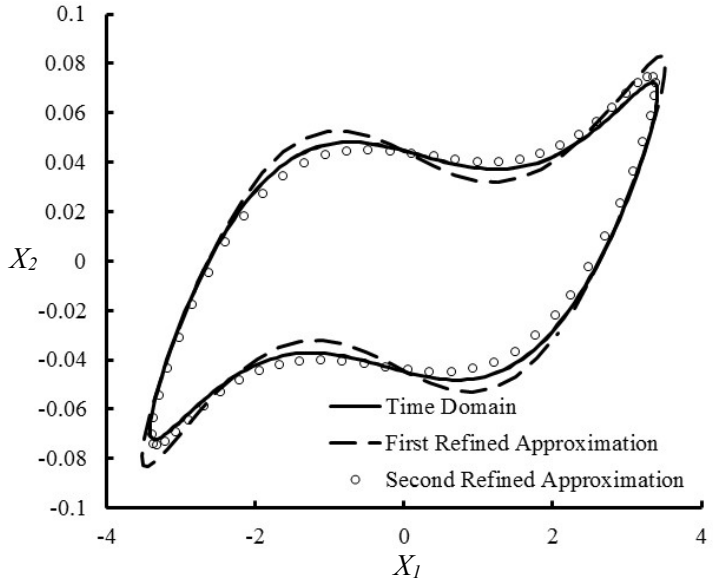

Fig. 4 Refined Stable Limit Cycle Prediction. K = 0.5, V = 6.9, C = 0, ε= 2.5 (Displacements)

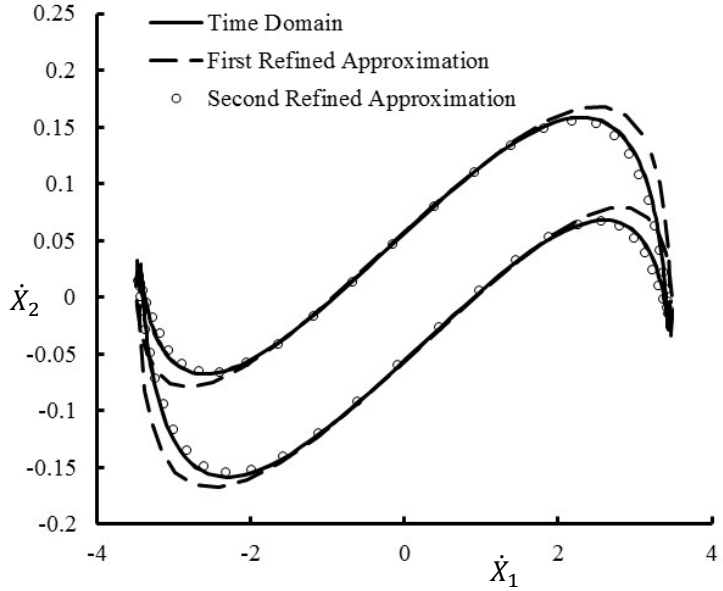

Fig. 5 Refined Stable Limit Cycle Prediction. K = 0.5, V = 6.9, C = 0, ε= 2.5 (Velocity Components)

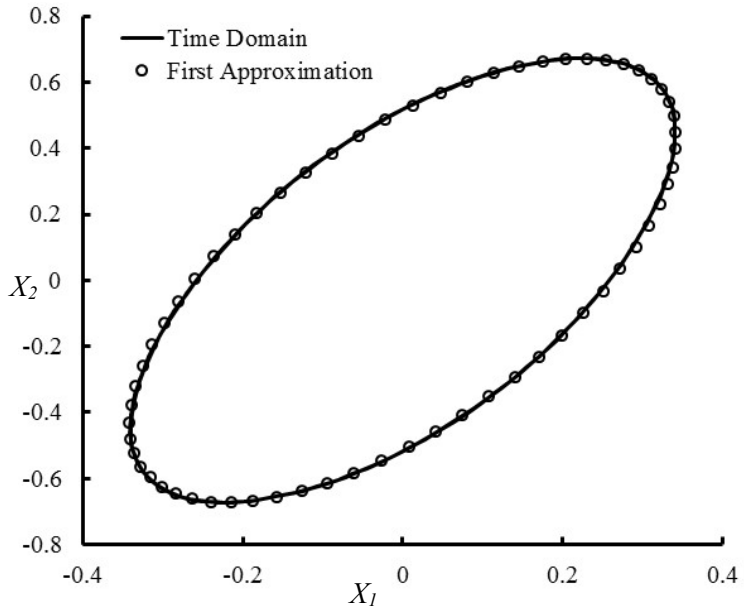

Fig. 6 First Approximation Unstable Limit Cycle Prediction. K = 0.5, V = 6.9, C = 0.1, ε= 2.5

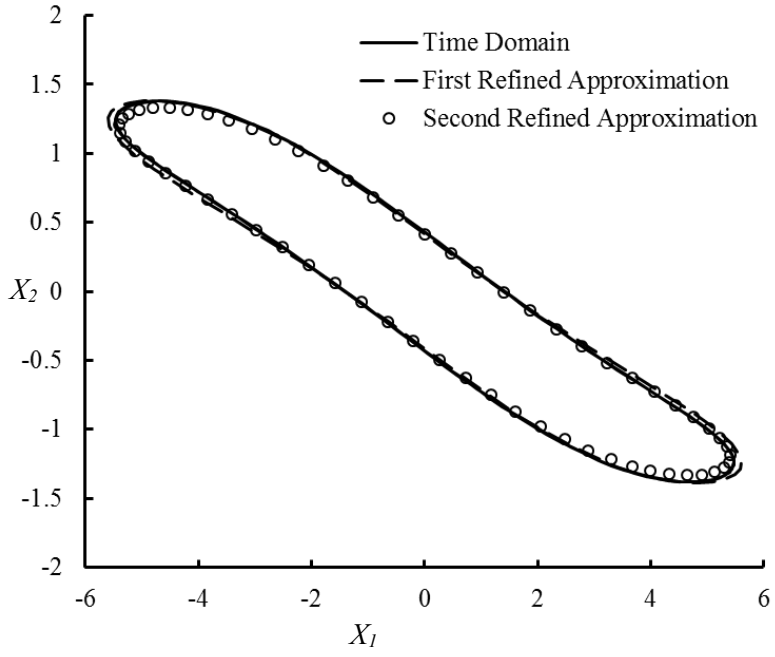

Fig. 7 Refined Stable Limit Cycle Prediction. K = 0.5, V = 6.9, C = 0.1, ε = 2.5 (Displacements)

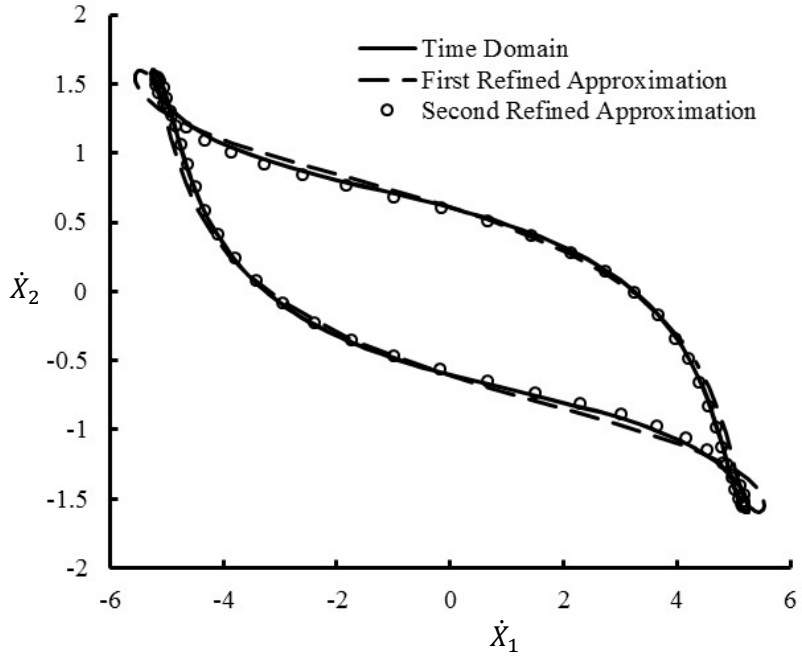

Fig. 8 Refined Stable Limit Cycle Prediction. $K = 0.5$, $V = 6.9$, $C = 0.1$, $\varepsilon = 2.5$ (Velocity Components)

As a further example, Figs. 9 and 10 show results for case $K = 4$, $V = 9$ and $C = 0$. The first refined approximation shows close agreement with time domain approximations and the second refined approximation gives yet closer agreement.

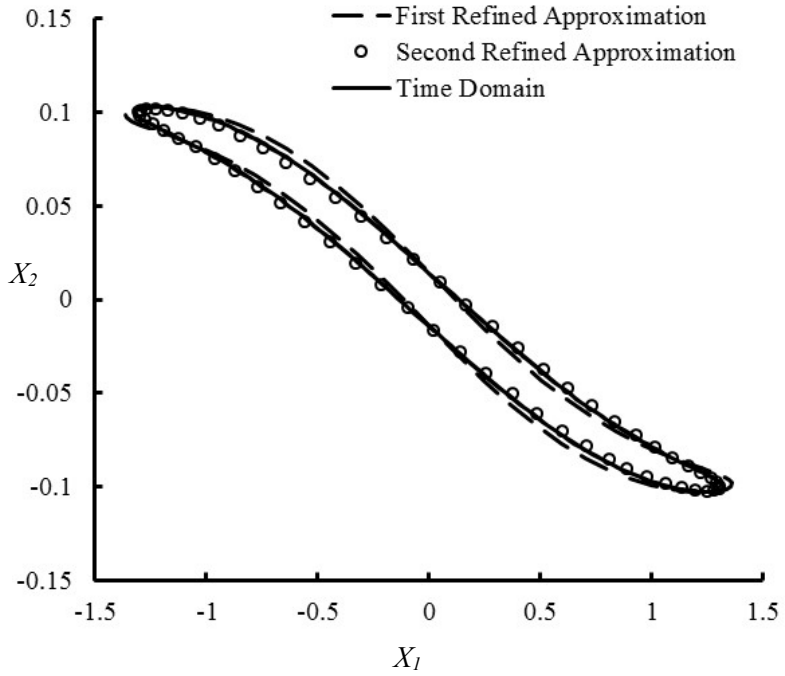

Fig. 9 Refined Stable Limit Cycle Prediction. $K = 4$, $V = 9$, $C = 0.0$, $\varepsilon = 2.5$ (Displacement Components)

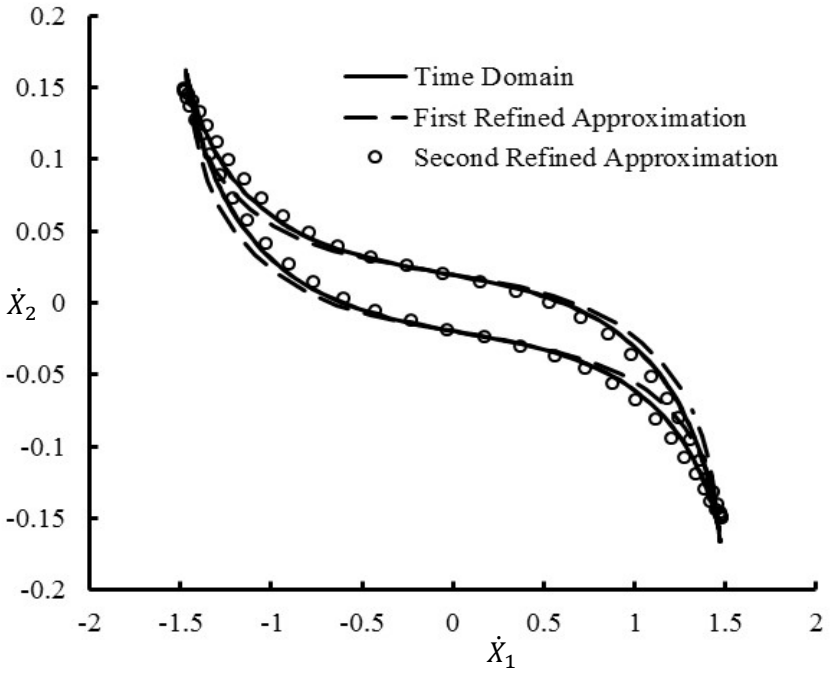

Fig. 10 **Refined Stable Limit Cycle Prediction. $K = 4$, $V = 9$, $C = 0.0$, $\varepsilon = 2.5$ (Velocity Components)**

Figs. 11 and 12 show stable limit cycle predictions for the case $K = 4$, $V = 9$, $C = 0.1$. Again, comparisons are made between time domain and the first and second refined approximation. Agreement is good and show the ability of the method to capture the effects of higher harmonics.

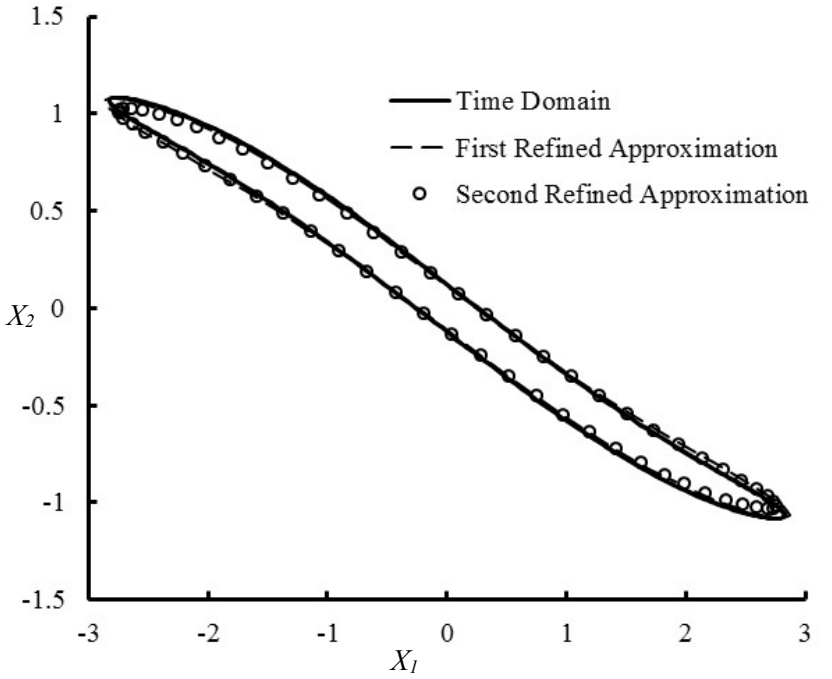

Fig. 11 **Refined Stable Limit Cycle Prediction. $K = 4$, $V = 9$, $C = 0.1$, $\varepsilon = 2.5$ (Displacement Components)**

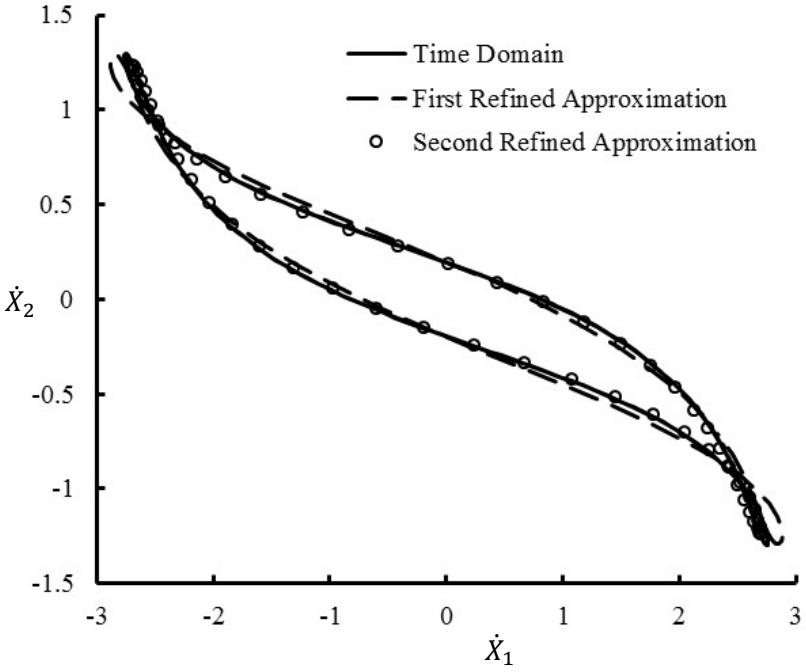

Fig. 12 **Refined Stable Limit Prediction. $K = 4$, $V = 9$, $C = 0.1$, $\varepsilon = 2.5$ (Velocity Components)**

7. Stability Domain Study

The bifurcation study shows how for the system described by equations (52) to (54) a subcritical Hopf bifurcation can occur whereby the unstable equilibrium point becomes stable and an unstable limit cycle appears. There is then associated with the stable equilibrium point a domain of attraction, the boundary of which is the stable manifold associated with the unstable limit cycle [36]. A local approximation to this stable manifold, and hence the domain of attraction, may then be determined as outlined in Section 5. It is emphasised that the resulting stability domains of attraction can only be anticipated to have any validity in the neighbourhood of the limit cycle. Nevertheless, this provides a way to indirectly further validate behaviour of the system predicted by the Floquet analysis.

A number of comparisons are now presented between stability domain predictions based on numerical integration of the system equations and based on Floquet analysis results using the method of Section 5. Points on the domain of attraction are determined in the time domain by a trial-and-error process. All the examples chosen are for conditions where the sub-critical Hopf bifurcation has just occurred.

Figs. 13 to 15 show stability domain estimates wherefor the case $\dot{X}_1 = 0$ and $\dot{X}_2 = 0$ for K between 4 and 6, $C = 0$, $\varepsilon = 2.5$ and V chosen such that bifurcation has just occurred in each case. It may be seen that agreement is good in all cases.

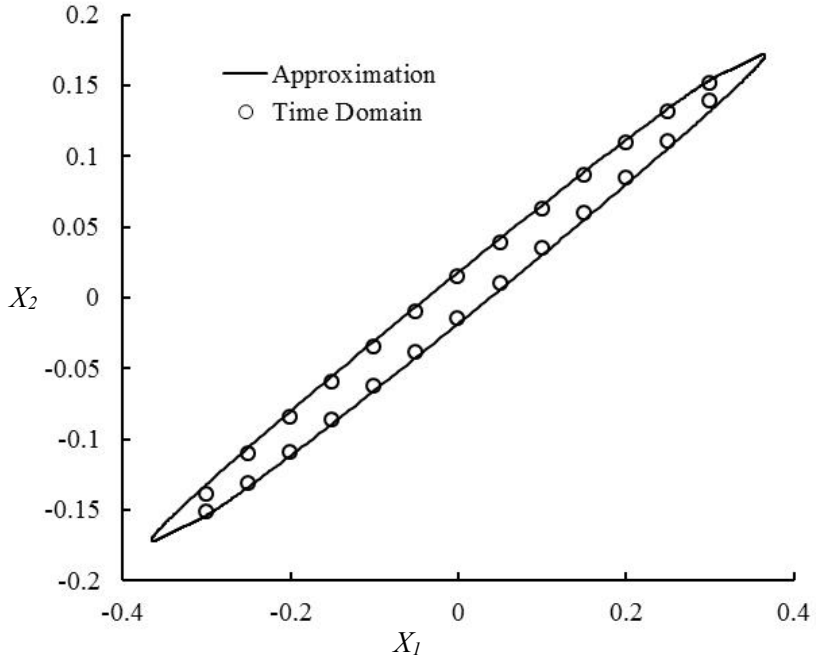

Fig. 13 Stability Domain for $K = 4$, $V = 7.32$, $\dot{X}_1=0$, $\dot{X}_2=0$

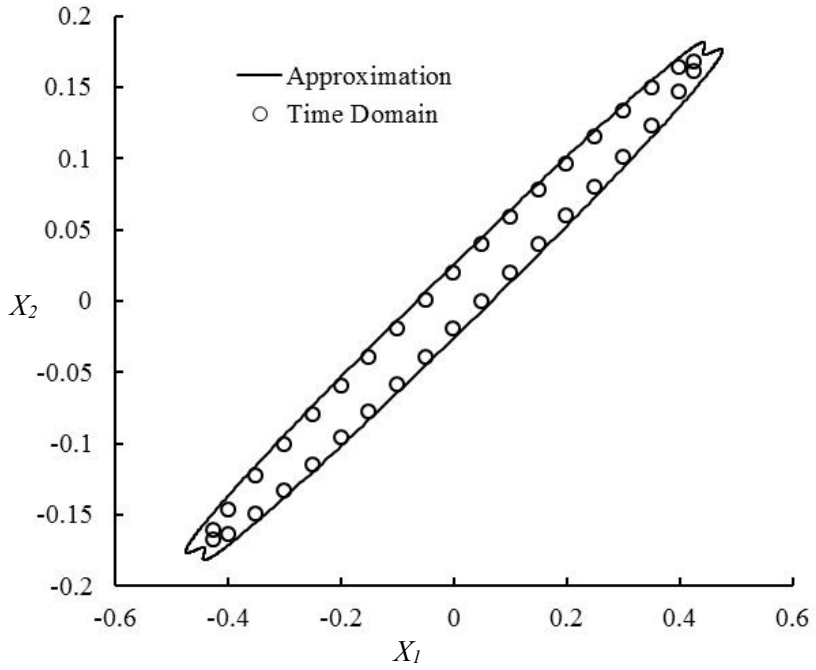

Fig. 14 Stability Domain for $K = 5$, $V = 6.67$, $\dot{X}_1=0$, $\dot{X}_2=0$

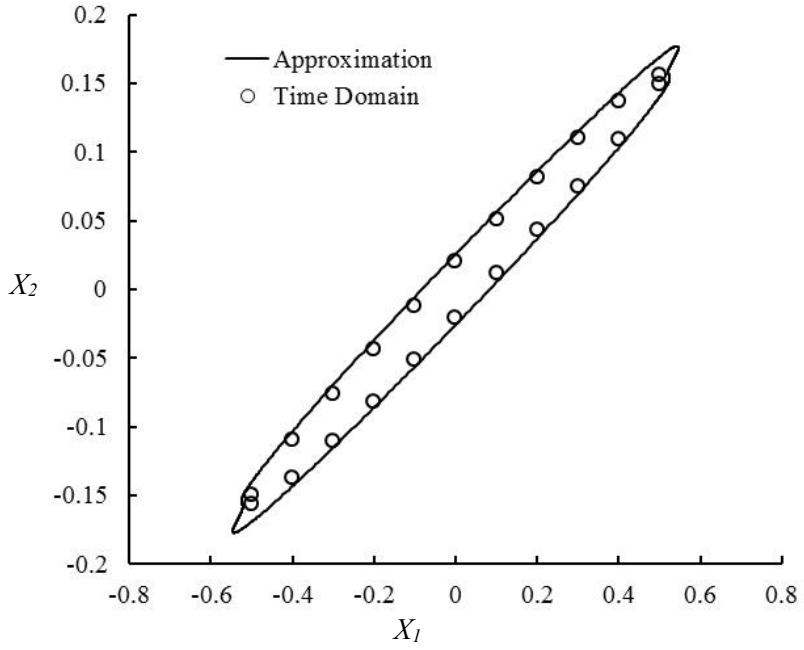

Fig. 15 Stability Domain for $K = 6$, $V = 6.24$, $\dot{X}_1=0$, $\dot{X}_2=0$

Figs. 16 to 18 show some further results for non-zero values of $\dot{X}_1$ and $\dot{X}_2$. Again the correspondence between the time domain results and predictions derived from the Floquet analysis are reasonable.

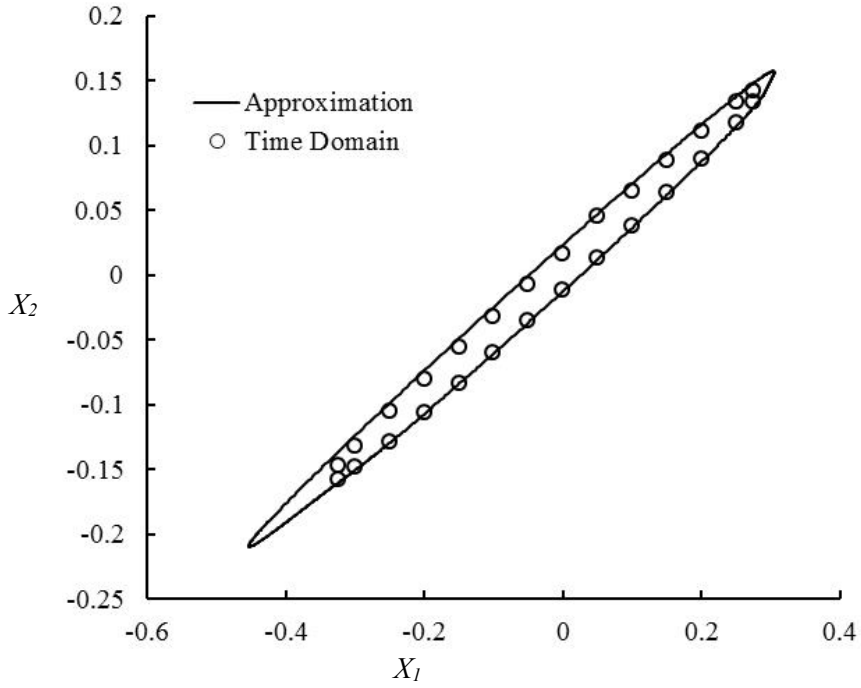

Fig. 16 Stability Domain for $K = 4$, $V = 7.32$, $\dot{X}_1=0.1$, $\dot{X}_2=0.05$

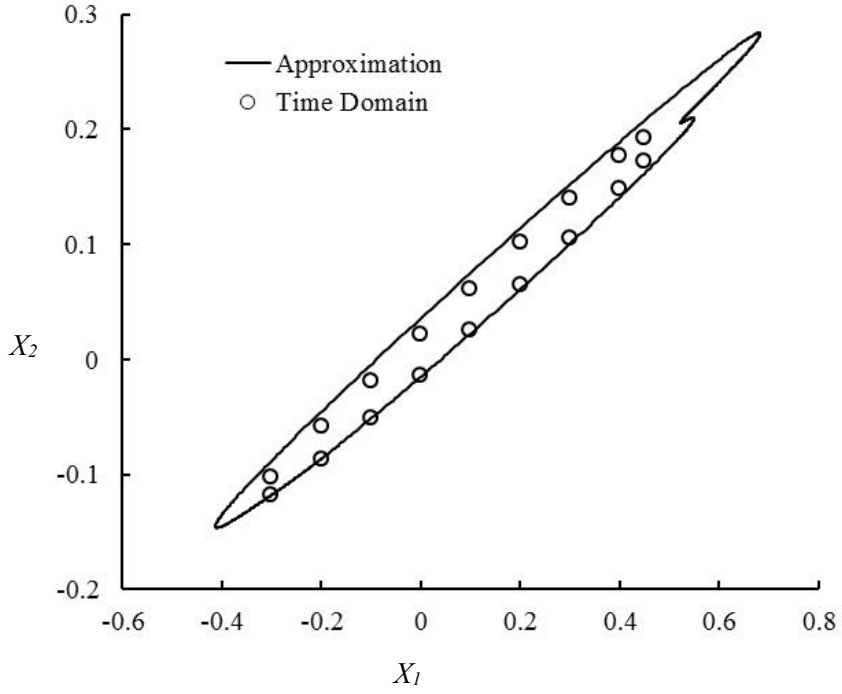

Fig. 17 Stability Domain for $K = 5$, $V = 6.67$, $\dot{X}_1$=0.17, $\dot{X}_2$=0.06

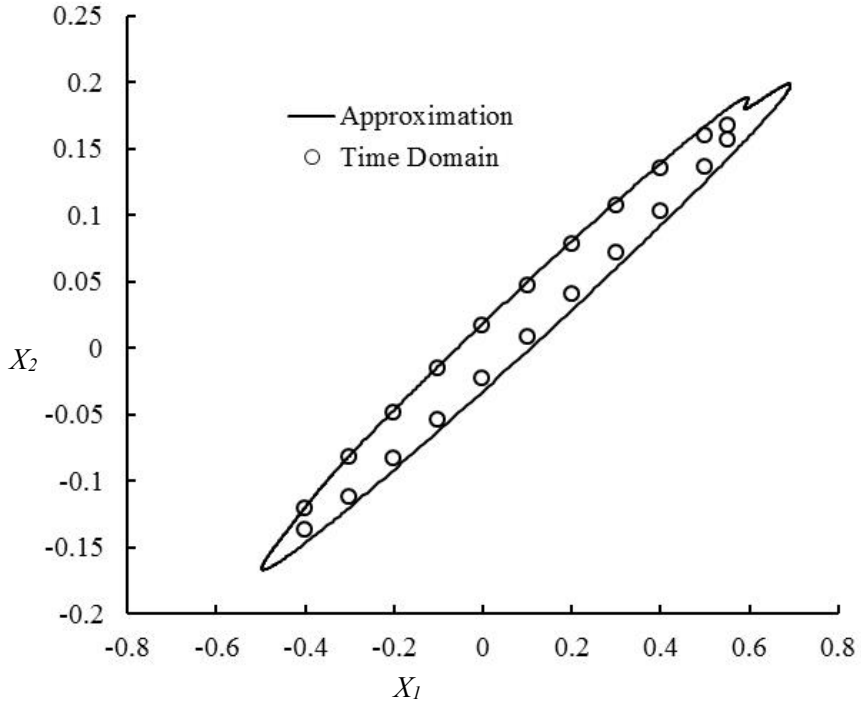

Fig. 18 Stability Domain for $K = 6$, $V = 6.24$, $\dot{X}_1$= -0.15, $\dot{X}_2$= -0.05

As noted in Section 4, the Floquet analysis is based on $\mathbf{\Delta X}$ being small compared to $\mathbf{X}$ in Equation (32). The results in Figs 13 to 18 were actually obtained subject to the condition:

$$\frac{|\mathbf{\Delta X}|}{A} < 1 \tag{55}$$

where A is the amplitude of the fundamental harmonic of the unstable limit cycle. It was therefore noticeable that for the cases considered, reasonable stability domain predictions could be obtained even when the smallness condition was relaxed.

8. Concluding Remarks

Analytical higher order approximations to limit cycles of an autonomous multi-degree-of-freedom system have been obtained using a method based on that of [30] and [31] and have been shown to give improved results over first approximation results which were identical to what would be obtained using harmonic balance based on the fundamental frequency component alone. Further iterations may be obtained in a similar manner resulting in higher order polynomial equations for A which would need to be solved numerically.

A method for carrying out Floquet analysis originally developed in [32] for a first order three degree-of-freedom system has been extended to a second order two-degree-of-freedom system. The method has then been used to provide some estimates of points on the boundary of the domain of attraction of the stable equilibrium point arising from, and just following, a sub-critical Hopf bifurcation. This is achieved by producing a local approximation to the stable manifold of the unstable limit cycle that arises.

The integro-differential equation to be solved for the limit cycles involves no approximations. These only arise through the iterative approach to its solution adopted here. Potentially it could form the basis for a numerical algorithm for limit cycle determination. In [32], the Floquet analysis was able to identify period doubling bifurcations in the analysis presented there. It might be expected that the extension used in the present work can do so also.

Although this study has focussed on cubic non-linearities, the method presented here could equally be used to refine limit cycle predictions for other non-linearity types arising in engineering applications. Furthermore, many non-linear aeroelastic analysis studies adopt a state-space representation for the unsteady aerodynamics, which is possible using reduced order models, as in [37], for example. The method presented here would be anticipated to be applicable in these cases also.

References

1. Nayfeh, A. H., Nayfeh AH. Perturbation methods. New York; Chichester;: Wiley; 1973
2. Nayfeh, Ali H., and Ali Hasan Nayfeh. Introduction to Perturbation Techniques, John Wiley & Sons, Incorporated, 1994. ProQuest Ebook Central, https://ebookcentral.proquest.com/lib/herts/detail.action?docID=696209.
3. Chan, H. S. Y., Chung, K. W., and Xu, Z., A Perturbation-Iterative Method for Determining the Limit Cycles of Strongly Non-Linear Oscillators, Journal of Sound and Vibration, Vol. 183, No. 4, pages 707-717, 1995.

4. Chan, H. S. Y., Chung, K. W., and Xu, Z., A Perturbation-Incremental Method for Strongly Non-Linear Oscillators, International Journal of Nonlinear Mechanics, Vol. 31, No. 1, pages 59-72, 1996.
5. Chung K. W., Chan C. L., Xu Z., Mahmoud G. M., A Perturbation-Incremental Method for Strongly Nonlinear Autonomous Oscillators with Many Degrees of Freedom. Nonlinear Dynamics, Vol. 28(3), pages 243-59, 2002.
6. Chung, K. W., Chan, C. L., Lee, B. H. K., Bifurcation analysis of a two-degree-of-freedom aeroelastic system with freeplay structural nonlinearity by a perturbation-incremental method, Journal of Sound and Vibration, Vol. 299, pages 520–539, 2007.
7. Liu, L, Dowell, E. H., Hall and K. C., A novel harmonic balance analysis for the Van Der Pol oscillator, International Journal of Nonlinear Mechanics, Vol. 42, pages 2-12, 2007.
8. Chen, Y. M. and Liu, J. K., Elliptic harmonic balance method for two degree-of-freedom self-excited oscillators, Communications in Nonlinear Science and Numerical Simulation, Vol. 14, pages 916-922, 2009.
9. Berci, M. and Dimitriadis, G., A combined Multiple Time Scales and Harmonic Balance approach for the transient and steady-state response of nonlinear aeroelastic systems, Journal of Fluids and Structures, Vol. 80, pages 132-144, 2018.
10. Dai, Honghua, Yue, Xiaokui, Yuan, Jianping, Xie, Dan, A fast harmonic balance technique for periodic oscillations of an aeroelastic airfoil, Journal of Fluids and Structures Vol 50, pages 231–252, 2014.
11. Dai, Honghua, Yue, Xiaokui, Yuan, Jianping, Xie, Dan, A time domain collocation method for studying the aeroelasticity of a two dimensional airfoil with a structural nonlinearity, Journal of Computational Physics, Vol 270, pages 214–237, 2014.
12. Dai, Honghua, Yue, Xiaokui, Yuan, Jianping, Xie, Dan, Dealiasing harmonic balance method for obtaining periodic solutions of an aeroelastic system, Aerospace Science and Technology, Vol. 77, pages 244–255, 2018.
13. Detroux, T., Renson, L., Masset, L., Kerschen, G., The harmonic balance method for bifurcation analysis of large-scale nonlinear mechanical systems, Computational Methods in Applied Mechanical Engineering, Vol. 296, pages 18–38, 2015.
14. Cochelin, B., Vergez, C., A high order purely frequency-based harmonic balance formulation for continuation of periodic solutions, Journal of Sound and Vibration, Vol. 324, pages 243-262, 2009.
15. Nui, Jiangchuan, Shen, Yongjun, Yang, Shaopu, Li Sujuan Li, Higher-order approximate steady-state solutions for strongly nonlinear systems by the improved incremental harmonic balance method, Journal of Vibration and Control, Vol. 24(16), pages 3744–3757, 2018.
16. Monfared, Z., Afsharnezhad, Z. and Esfahani, J., Flutter, limit cycle oscillation, bifurcation and stability regions of an airfoil with discontinuous freeplay nonlinearity, Nonlinear Dynamics, Vol. 90, Part 3, Issue 3, pages 1965-1986, 2017.
17. Liping, L., Dowell, E. H., Thomas, J. P., Higher Order Harmonic Balance Analysis for Limit Cycle Oscillations in an Airfoil with Cubic Restoring Forces, AIAA 2005-1918, 46th AIAA/ASME/ASCE/AHS/ASC Structures, Structural Dynamics & Materials Conference, 18 - 21 April 2005, Austin, Texas.
18. Lee, B. H. K., Liu, L, Chung, K. W., Airfoil motion in subsonic flow with strong cubic nonlinear restoring forces, Journal of Sound and Vibration, Vol. 281, pages 699-717, 2005.
19. Liu, L., Dowell, E. H., The Secondary Bifurcation of an Aeroelastic Airfoil Motion: Effect of High Harmonics, Nonlinear Dynamics, Vol. 37, pages 31–49, 2004.
20. Kim, S-H, Lee, I, Aeroelastic Analysis of a flexible airfoil with a freeplay non-linearity, Journal of Sound and Vibration, Vol. 193(4), pages 823-846, 1996.
21. Raghothama, A., Narayanan, S. Non-linear dynamics of a two-dimensional airfoil by incremental harmonic balance method, Journal of Sound and Vibration, Vol. 226(3), pages 493-517, 1999.

22. Padmanabhan, M.A., Dowell, E.H., Thomas, J.P., Pasiliao, C.L., Store-induced limit-cycle oscillations due to nonlinear wing-store attachment, Journal of Aircraft, Vol. 53 (3), pages. 778-789, 2016.
23. Liu, L., Dowell, E.H., High dimensional harmonic balance analysis for dynamic piecewise aeroelastic systems, ASME International Mechanical Engineering Congress and Exposition, Proceedings, 12, pages 659-669, 2009.
24. Liu, L., Dowell, E.H., Thomas, J.P., A high dimensional harmonic balance approach for an aeroelastic airfoil with cubic restoring forces, Journal of Fluids and Structures, 23(3), pages 351-363, 2007.
25. Liu, L., Dowell, E.H., Thomas, J.P., Higher order harmonic balance analysis for limit cycle oscillations in an airfoil with cubic restoring forces, Collection of Technical Papers - AIAA/ASME/ASCE/AHS/ASC Structures, Structural Dynamics and Materials Conference, 3, pages 1467-1476. 2005.
26. Irani, Saied, Sarrafzadeh, Hamid, Amoozgar, Mohammad Reza, Bifurcation in a 3-DOF Airfoil with Cubic Structural Nonlinearity, Chinese Journal of Aeronautics, Vol. 24, pages 265-278, 2011.
27. Xuechuan W, Xiaokui Y, Honghua D, Jianping Y, Analysis of a Two-Dimensional Aeroelastic system Using the Differential Transform Method, Journal of Computational nonlinear dynamics, 2016.
28. Moore, G., Floquet Theory as a Computational Tool, SIAM Journal of Numerical Analysis, Vol. 42, No. 6, pp. 2522–2568, 2005.
29. Qian, Y. H. and Zhang, Y. F., Optimal extended homotopy analysis for Multi-Degree-of-Freedom nonlinear dynamical systems and its application, Structural Engineering and Mechanics, Vol. 61, No. 1, pages 105-116, 2017.
30. Schmidt G, Tondl A., Non-linear vibrations. Cambridge: Cambridge University Press; 1986.
31. Schmidt G, Schulz. R, Parametererregte Schwingungen, Berlin: Deutscher Verl. der Wissenschaften, 1975.
32. Bonani, F. and Gilli, M, Analysis of Stability and Bifurcations of Limit Cycles in Chua's Circuit Through the Harmonic Balance Approach, IEEE Transactions on Circuits and Systems – I: Fundamental Theory and Applications, Vol. 46, No. 8, August 1999.
33. Whittaker, E. T., Watson, G. N., A Course in Modern Analysis, Cambridge University Press, pages 413 – 416, 1996.
34. Ashley, H., Zartarian, G., Piston Theory – a New Aerodynamic Tool for the Aeroelastician, Journal of the Aeronautical Sciences, Vol. 23, pages 1109-1118, 1956.
35. Hu, H., Tang, J. H., A convolution integral method for certain strong nonlinear oscillators, Journal of Sound and Vibration, Vol. 285, pages 1235-1241, 2005.
36. Venkatasubramanian, V. and Ji, W., Numerical Approximation of (n-1)-Dimensional Stable Manifolds in Large Systems such as Power Systems, *Automatica* **10**, 1877-1883, 1997.
37. Gai, Guanqun, Timme, Sebastian, Nonlinear reduced-order modelling for limit-cycle oscillation analysis, Nonlinear Dynamics, Vol. 84, pages 991–1009, 2016.
38. A. Simpson, An Algorithm for Autonomous Non-Linear Dynamical Equations. Aeronautical Quarterly, pages 211-233, 1977.

APPENDIX A Determination of the Matrices G_k in Equation (35)

The coefficients $\mathbf{G}_k$ in Equation (35) may be found by from a Fourier expansion of:

$$f'(r^T X) = 3K(r^T X)^2 \tag{A1}$$

with $\mathbf{X}$ given by Equation (31). This Fourier expansion will be of the form:

$$f'(\mathbf{r^T X}) = 3K\left\{U_0 + \sum_{k=2}^{\infty} U_{c2} cos2k\tau + \sum_{k=2}^{\infty} U_{s2} sin2k\tau\right\} \tag{A2}$$

Noting that as $\mathbf{r^T X}$ has a Fourier series in odd terms, $f'(\mathbf{r^T X})$ will therefore have an expansion in even terms. As the right hand side of Equation (35) is expressed in complex form, the following equations then result for the matrices $\mathbf{G}_{2k}$, $\mathbf{G}_{-2k}$, $\mathbf{G}_0$:

$$\begin{aligned} \mathbf{G}_0 &= 3K\varepsilon \mathbf{s}\mathbf{r}^T U_o \\ \mathbf{G}_{2k} &= \frac{3}{2} K\varepsilon \mathbf{s}\mathbf{r}^T \left\{U_{c2} + \frac{U_{s2}}{i}\right\} \\ \mathbf{G}_{-2k} &= \frac{3}{2} K\varepsilon \mathbf{s}\mathbf{r}^T \left\{U_{c2} - \frac{U_{s2}}{i}\right\} \end{aligned} \tag{A3}$$

for $k = 1, 2, 3, \ldots$.

APPENDIX B Determination of Residues of $\mathrm{Det}\{\widetilde{\boldsymbol{G}}_{\mathbf{0}}^{-\mathbf{1}}\}$.

These may be found in the following way. First, note that from Equation (39), $\widetilde{\mathbf{G}}_0$ may be written:

$$\widetilde{\mathbf{G}}_0 = \lambda^2 \mathbf{I} + \lambda \mathbf{G} + \mathbf{H} + \mathbf{s}\mathbf{r}^T \mathbf{G}_0 \tag{B1}$$

Now write:

$$\mathbf{U} = \begin{bmatrix} -\mathbf{H} - \mathbf{s}\mathbf{r}^T \mathbf{G}_0 & \mathbf{0} \\ \mathbf{0} & \mathbf{I} \end{bmatrix} \tag{B2}$$

$$\boldsymbol{V} = \begin{bmatrix} \mathbf{0} & -\mathbf{H} - \mathbf{s}\mathbf{r}^T \mathbf{G}_0 \\ -\mathbf{H} - \mathbf{s}\mathbf{r}^T \mathbf{G}_0 & -\mathbf{G} \end{bmatrix} \tag{B3}$$

Then $\lambda_{s1}, \lambda_{s2}, \lambda_{s3}, \lambda_{s4}$ will also be solutions to the eigenvalue problem:

$$\mathbf{V}\begin{bmatrix} \boldsymbol{\chi} \\ \lambda\boldsymbol{\chi} \end{bmatrix} = \lambda \mathbf{U}\begin{bmatrix} \boldsymbol{\chi} \\ \lambda\boldsymbol{\chi} \end{bmatrix} \tag{B4}$$

Defining $\boldsymbol{\Lambda} = \mathrm{diag}[\lambda_{s1} \quad \lambda_{s2}]$, left-hand and right-hand eigenvector matrices of (B4), $\bar{\mathbf{L}}$, $\bar{\mathbf{R}}$ may be written:

$$\bar{\mathbf{L}} = \begin{bmatrix} \mathbf{L} & \boldsymbol{\Lambda}\mathbf{L} \\ \mathbf{L}^* & \boldsymbol{\Lambda}^*\mathbf{L}^* \end{bmatrix} \tag{B5}$$

$$\bar{\mathbf{R}} = \begin{bmatrix} \mathbf{R} & \mathbf{R}^* \\ \mathbf{R}\boldsymbol{\Lambda} & \mathbf{R}^*\boldsymbol{\Lambda}^* \end{bmatrix} \tag{B6}$$

Where $\bar{L}$ and $\bar{R}$ are normalised such that:

$$\bar{\mathbf{L}}\mathbf{U}\bar{\mathbf{R}} = \mathbf{I} \tag{B7}$$

It is then possible to write the inverse of a matrix of the type in (B1) as [38]:

$$\widetilde{\mathbf{G}}_0^{-1} = [\lambda^2\mathbf{I} + \lambda\mathbf{G} + \mathbf{H} + \mathbf{s}\mathbf{r}^T\mathbf{G}_0]^{-1} = [\mathbf{L} \quad \mathbf{L}^*] \begin{bmatrix} [\lambda\mathbf{I} - \boldsymbol{\Lambda}]^{-1} & 0 \\ 0 & [\lambda\mathbf{I} - \boldsymbol{\Lambda}^*]^{-1} \end{bmatrix} \begin{bmatrix} \boldsymbol{\Lambda}\mathbf{R} \\ \boldsymbol{\Lambda}^*\mathbf{R}^* \end{bmatrix} \tag{B8}$$

The residues R_1, R_2, R_3, R_4 of $\mathrm{Det}\{\widetilde{\mathbf{G}}_0^{-1}\}$ for each of λ_{s1} λ_{s2} λ_{s3} λ_{s4} may then be found by expanding the determinant and may be written:

$$R_1 = \sum_{k=2,3,4} \begin{vmatrix} \bar{L}_{11} & \bar{L}_{1k} \\ \bar{L}_{21} & \bar{L}_{2k} \end{vmatrix} \begin{vmatrix} \bar{R}_{11} & \bar{R}_{12} \\ \bar{R}_{k1} & \bar{R}_{k2} \end{vmatrix} \frac{1}{(\lambda_{sk} - \lambda_{s1})} \tag{B9}$$

$$R_2 = \sum_{l=1,3,4} \begin{vmatrix} \bar{L}_{12} & \bar{L}_{1k} \\ \bar{L}_{22} & \bar{L}_{2k} \end{vmatrix} \begin{vmatrix} \bar{R}_{21} & \bar{R}_{22} \\ \bar{R}_{k1} & \bar{R}_{k2} \end{vmatrix} \frac{1}{(\lambda_{sk} - \lambda_{s2})} \tag{B10}$$

$$R_3 = \sum_{l=1,2,4} \begin{vmatrix} \bar{L}_{13} & \bar{L}_{1k} \\ \bar{L}_{23} & \bar{L}_{2k} \end{vmatrix} \begin{vmatrix} \bar{R}_{31} & \bar{R}_{32} \\ \bar{R}_{k1} & \bar{R}_{k2} \end{vmatrix} \frac{1}{(\lambda_{sk} - \lambda_{s3})} \tag{B11}$$

$$R_4 = \sum_{l=1,2,3} \begin{vmatrix} \bar{L}_{14} & \bar{L}_{1k} \\ \bar{L}_{24} & \bar{L}_{2k} \end{vmatrix} \begin{vmatrix} \bar{R}_{41} & \bar{R}_{42} \\ \bar{R}_{k1} & \bar{R}_{k2} \end{vmatrix} \frac{1}{(\lambda_{sk} - \lambda_{s4})} \tag{B12}$$

from which the residues c_1, c_2, c_3, c_4 *i*n Equation (42) may be determined.

Appendix C Determination of Coefficients of Equation (45)

The coefficients *a*, *b*, *c*, *d* of Equation (45) for the Floquet multipliers are given by the following equations:

$$\begin{aligned} a = &- c_1\mu_{s1}\mu_{s2}\mu_{s3}\mu_{s4}(\mu_{s2} - 1)(\mu_{s3} - 1)(\mu_{s4} - 1) \\ &- c_2\mu_{s1}\mu_{s2}\mu_{s3}\mu_{s4}(\mu_{s1} - 1)(\mu_{s3} - 1)(\mu_{s4} - 1) \\ &- c_3\mu_{s1}\mu_{s2}\mu_{s3}\mu_{s4}(\mu_{s1} - 1)(\mu_{s2} - 1)(\mu_{s4} - 1) \\ &- c_4\mu_{s1}\mu_{s2}\mu_{s3}\mu_{s4}(\mu_{s1} - 1)(\mu_{s2} - 1)(\mu_{s3} - 1) \end{aligned} \tag{C1}$$

$$\begin{aligned} b = &\, c_1\mu_{s1}(\mu_{s2} - 1)(\mu_{s3} - 1)(\mu_{s4} - 1)(\mu_{s2}\mu_{s3} + \mu_{s3}\mu_{s4} + \mu_{s4}\mu_{s2}) \\ &+ c_2\mu_{s2}(\mu_{s1} - 1)(\mu_{s3} - 1)(\mu_{s4} - 1)(\mu_{s1}\mu_{s3} + \mu_{s1}\mu_{s4} + \mu_{s4}\mu_{s3}) \\ &+ c_3\mu_{s3}(\mu_{s1} - 1)(\mu_{s2} - 1)(\mu_{s4} - 1)(\mu_{s1}\mu_{s2} + \mu_{s2}\mu_{s4} + \mu_{s4}\mu_{s1}) \\ &+ c_4\mu_{s4}(\mu_{s1} - 1)(\mu_{s2} - 1)(\mu_{s3} - 1)(\mu_{s1}\mu_{s2} + \mu_{s2}\mu_{s3} + \mu_{s4}\mu_{s3}) \end{aligned} \tag{C2}$$

$$
\begin{aligned}
c = &- c_1\mu_{s1}(\mu_{s2}-1)(\mu_{s3}-1)(\mu_{s4}-1)(\mu_{s2}+\mu_{s3}+\mu_{s4}) \\
&-c_2\mu_{s2}(\mu_{s1}-1)(\mu_{s3}-1)(\mu_{s4}-1)(\mu_{s1}+\mu_{s3}+\mu_{s4}) \\
&- c_3\mu_{s3}(\mu_{s1}-1)(\mu_{s2}-1)(\mu_{s4}-1)(\mu_{s1}+\mu_{s2}+\mu_{s4}) \\
&- c_4\mu_{s4}(\mu_{s1}-1)(\mu_{s2}-1)(\mu_{s3}-1)(\mu_{s1}+\mu_{s2}+\mu_{s3})
\end{aligned} \tag{C3}
$$

$$
\begin{aligned}
d = &\, c_1\mu_{s1}(\mu_{s2}-1)(\mu_{s3}-1)(\mu_{s4}-1) + c_2\mu_{s2}(\mu_{s1}-1)(\mu_{s3}-1)(\mu_{s4}-1) \\
&+c_3\mu_{s3}(\mu_{s1}-1)(\mu_{s2}-1)(\mu_{s4}-1) + c_4\mu_{s4}(\mu_{s1}-1)(\mu_{s2}-1)(\mu_{s3}-1)
\end{aligned} \tag{C4}
$$